

PAPER

Ground Test of Radio Frequency Compatibility for Cn-Band Satellite Navigation and Microwave Landing System

Ruihua LIU[†], Yin LI[†], Ling ZOU[†], and Yude NI^{†a)}, *Nonmembers*

SUMMARY Testing the radio frequency compatibility between Cn-band Satellite Navigation and Microwave Landing System (MLS) has included establishing a specific interference model and reporting the effect of such interference. This paper considers two interference scenarios according to the interfered system. By calculating the Power Flux Density (PFD) values, the interference for Cn-band satellite navigation downlink signal from several visible space stations on MLS service is evaluated. Simulation analysis of the interference for MLS DPSK-data word signal and scanning signal on Cn-band satellite navigation signal is based on the Spectral Separation Coefficient (SSC) and equivalent Carrier-to-Noise Ratio methodologies. Ground tests at a particular military airfield equipped with MLS ground stations were successfully carried out, and some measured data verified the theoretical and numerical results. This study will certainly benefit the design of Cn-band satellite navigation signals and guide the interoperability and compatibility research of Cn-band satellite navigation and MLS.

key words: *radio frequency compatibility, Cn-band satellite navigation signal, Microwave Landing System, ground tests, measured data*

1. Introduction

As a new navigation band with application potential, Cn-band (5,010 MHz~5,030 MHz), was officially allocated by the International Telecommunication Union (ITU) for satellite navigation downlink signals in 2,000 [1], [2]. Since then, researchers, represented by the United States and the European Space Agency, have conducted much in-depth research on the technology and performance of Cn-band navigation signals [3]–[5]. The results show that the new satellite navigation band has significant advantages: the Cn-band signal has excellent resistance to ionospheric delay and multipath effects, and its UHF characteristics leave a rich margin for antenna design [6], [7]. However, its advantages are opposed to the high spaceborne payload requirements that cannot be ignored [8]. This means that to put the Cn-band into a formal application, a very high modification cost has to be paid, which puts high pressure on the technology level.

Paper [9] summarizes the general characteristics of Cn-band satellite navigation signals, points out the difficulties in applying Cn-band navigation signals and gives ideas on how to solve these difficulties. The research on the satellite navigation system in this band, mainly concentrated on the signal modulation method and signal reception performance,

is already abundant.

With the increasing congestion of L-band satellite navigation signals, the compatible operation of L-band satellite navigation signals faces difficulties. The research on Cn-band satellite navigation has started to be actively promoted, and the array antenna and other technologies developed at high speed in recent years have provided the possibility for the practical application of Cn-band satellite navigation signals. The China Area Positioning System (CAPS), independently developed by the Chinese Academy of Sciences, is a transponder-style satellite navigation system that broadcasts C-band downlink signals and is well suited to carry feasibility studies on Cn-band satellite navigation signals [10]. Scholars represented by Jian Ge, Xiaochun Lu, and Xue Wang of the Chinese Academy of Sciences have made much research on the design and performance of Cn-band satellite navigation signals [11], [12].

The upper sideband of the Cn-band, 5,030 MHz to 5,150 MHz, has been dominated by the international standard Microwave Landing System (MLS). Before standardizing the application of Cn-band signals, the spectrum compatibility of these two systems must be tested and analyzed. Mancang Niu [13] and Mehong Liu [14], [15] of Shanghai Jiao Tong University, China, have conducted simulations for the interference caused by C-band satellite navigation signals using various modulation methods to MLS, based on the protection guidelines for MLS service made by the International Civil Aviation Organization (ICAO).

Up to today, the analysis of radio frequency compatibility between satellite navigation and MLS in Cn-band stays at the stage of simulation analysis, and only the interference of navigation signal to MLS is analyzed. In this paper, we first verify whether the aggregate Power Flux Density (PFD) of downlink signals transmitted by several visible Cn-band satellites falling within the MLS band exceeds the protection threshold. Then, we use the spectral separation coefficient (SSC) and the equivalent carrier-to-noise ratio method [16], to evaluate the impact of MLS signals on the reception of Cn-band satellite navigation downlink signals. The above studies are based on the navigation signal and MLS signal data collected at a military airport, and the real situation of the radio frequency compatibility of the two systems is obtained by comparing the simulation analysis with the actual measurement results.

The paper is organized as follows. The system characteristics of Cn-band satellite navigation and MLS are given in Sect. 2. The method of radio frequency compatibility

Manuscript received February 11, 2022.

Manuscript publicized May 19, 2022.

[†]The authors are with College of Electronic Information and Automation, Civil Aviation University of China, Tianjin 300300, China.

a) E-mail: yudeni_cauc@sina.com

DOI: 10.1587/transcom.2022EBP3021

analysis of the two systems is given in Sect. 3. The implementation of the compatibility test and the test results are explained in detail in Sect. 4. Finally, Sect. 5 concludes this paper.

2. System Characteristics

2.1 Cn-Band Satellite Navigation Signal Characteristics

The modulation method of satellite navigation signal directly affects the performance of satellite navigation system service, in which the carrier used for navigation signal and the selection of carrier frequency are crucial [17]. On the one hand, according to the rationale of satellite navigation signal generation, it is not difficult to conclude that the carrier frequency must be an integer multiple of the clock reference frequency of 1.023 MHz. To obtain a better out-of-band rejection performance, BPSK(*n*) modulation can be used, where “*n*” indicates that the code rate is $n \cdot 1.023$ MHz. The “*n*” is taken to be no more than 10 to retain the maximum signal main lobe energy, considering that the bandwidth of the Cn-band is only 20 MHz [18], [19]. On the other hand, to leave enough protection margin for the adjacent band primary system, i.e., MLS, paper [20] pointed out that the choice of 5022.93 MHz as the carrier frequency of the navigation signal can meet the requirements stated above.

This analysis assumes a Cn-band satellite navigation signal $s(t)$ with a carrier frequency f_c of 5022.93 MHz and modulation methods of BPSK(2), BPSK(5), and BPSK(10), respectively. We have:

$$s(t) = s_I(t) \cos(2\pi f_c t) + s_Q(t) \sin(2\pi f_c t) \quad (1)$$

Where $s_I(t)$ and $s_Q(t)$ are the pseudo-random code sequences of I-way and Q-way, respectively.

The signal has power spectrum $S_{BPSK}(f)$ is then:

$$S_{BPSK}(f) = T_c \text{sinc}^2(\pi f T_c) \quad (2)$$

In Eq. (2), T_c is the duration of a code piece. Figure 1 shows the power spectrum of the satellite navigation signal with three modulation methods, BPSK(2), BPSK(5), and BPSK(10), and a carrier frequency of 5022.93 MHz.

The downlink of a Cn-band satellite navigation system, as shown in Fig. 2, operates in a band adjacent to the MLS operating band, and its transmitted downlink signal may cause harmful interference to the MLS service.

The satellite navigation downlink signal in Fig. 2 can be considered as propagating in free-space. The empirical Eq. (3) is used to calculate the transmission loss L_f of the downlink signal.

$$L_f = 32.44 + 20 \lg d + 20 \lg f \quad (3)$$

Where: d is the distance from the satellite to the Earth’s surface in km; f is the satellite navigation downlink frequency in MHz.

Then the satellite signal power P_r received by an antenna at point r on the ground is [21]:

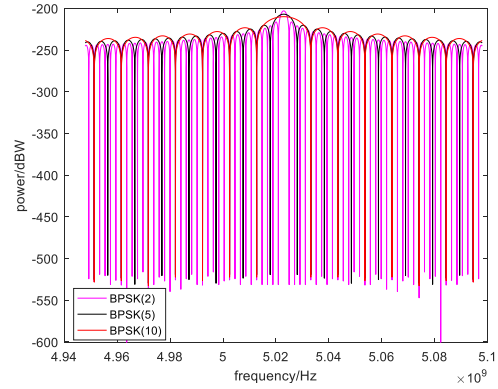


Fig. 1 Theoretical PSD of navigation signal.

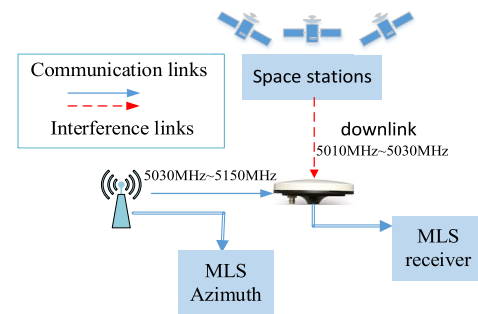


Fig. 2 Scenario for satellite navigation signal interference to MLS service.

$$P_r = P_t + G_t + G_r + L_f - L_{atm} \quad (4)$$

Where: P_r and P_t unit of dBW or dBm; G_t for the gain of the satellite transmitting antenna; G_r for the receiving antenna gain used to receive signals in dBi; L_{atm} represents the value of about 2 dB of atmospheric loss.

The satellite navigation signal is circularly polarized and the signal power can be calculated from the above link propagation model, usually, the power of the satellite signal arriving at a point on the ground is around -130 dBm to -120 dBm, depending on the satellite position.

2.2 MLS Characteristics

The MLS is a precision approach system based on the time-based beam scanning principle, adopted by ICAO to provide all-weather approach services for civilian airports and air bases, even under adverse weather conditions. The mobile MLS (MMLS) is also widely used in the landing of fighter aircraft, carrier aircraft, missile precision strikes, and military equipment formation movement [22]. Figure 3 shows the layout of a typical MLS and the data transmission link. The figure includes the main guidance signal transmissions in the sector covered by the MLS azimuth station signals and the ranging signals emitted by the P/DME equipment.

As can be seen from Fig. 3, a typical MLS ground equipment layout includes an azimuth station, an elevation station, and a precision DME. The azimuth and elevation stations operate on more than 200 channels in the frequency band

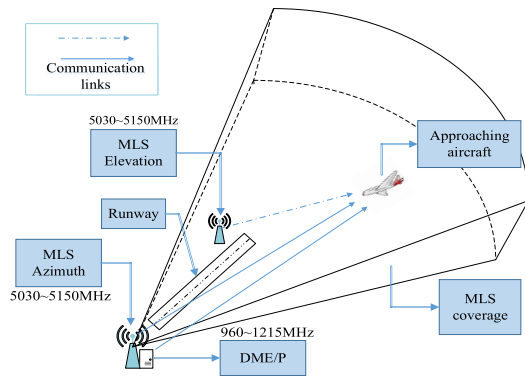


Fig. 3 Ground equipment arrangement of MLS and data link.

of 5,030 MHz to 5,150 MHz and broadcast the differential phase-shift keying (DPSK) data word signal with synchronization and other information, as well as the scanning signal for the aircraft to determine its angular position, while the distance information is provided by the precision DME operating at 960 MHz~1,215 MHz.

The MLS broadcasts two kinds of signals. The DPSK data word signal uses the coding rules specified by ICAO, with a code rate of 15,625 Hz, and its power spectrum is consistent with the general DPSK signal. The scanning signal is formed by the array antenna assignment, and the 3 dB beamwidth (1° , 2° or 3° is generally used for azimuth antenna, depending on the runway length) of the scanning antenna pattern is defined as

$$A(\theta) = e^{-k\left(\frac{\theta}{Bw}\right)^2} \quad (5)$$

In Eq. (5), $k = \ln 2$, the value range for θ is $-62^\circ \sim +62^\circ$ for azimuth antenna.

The “TO” and “FRO” scan pulse envelope is regarded as a reflection of the pattern of the scanning antenna on the time axis [23], combined with the MLS scanning signal angle measurement principle, the time-domain expression of scanning signal $f(t)$ can be obtained as

$$f(t) = e^{-k\left(\frac{vt}{Bw}\right)^2} \quad (6)$$

Where: v is the scanning rate, for the azimuth generally $20^\circ/\text{ms}$.

Assuming that the terrain around the runway is flat, and there are no obvious obstacles in the MLS guidance signal coverage sector, the interference scenario shown in Fig. 4 is established to evaluate the interference of MLS service signals to the Cn-band satellite navigation downlink service.

Except for the DME/P, all the MLS ground equipment providing approach service to the aircraft on a runway operate on the same frequency point and have the same signal transmission model. Take the azimuth approach guidance signal as an example, the MLS signal power at a certain point in the coverage is calculated by the following equation:

$$P_R = P_T + G_T + G_R - C_l - P_L \quad (7)$$

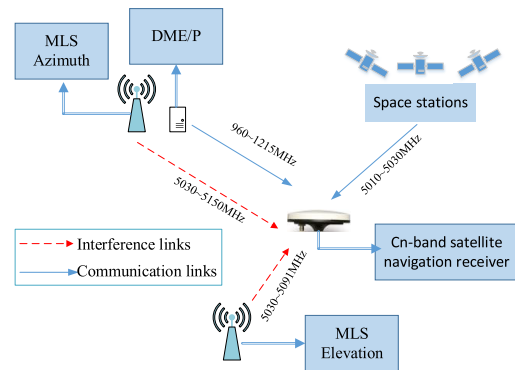


Fig. 4 Scenario for MLS signal interference to satellite navigation service.

Table 1 Parameters for MLS signal power estimating.

Parameters	MLS signal	
	DPSK signal	Scanning signal
frequency/MHz	5,030~5,150	
bandwidth/kHz	300	
transmit power/dBm	46	
antenna gain/dBi	8~0	23~16
polarization loss/dB	3	
cable loss/dB	2	
other loss/dB		
atmospheric loss	0.3	0.3
rainfall	2.2	2.2
horizontal multipath	3.0	0.5
vertical multipath	2.0	2.0

Where: P_T is the MLS transmit power in dBW or dBm, G_T is the transmit antenna gain, G_R is the receive antenna gain in dBi, C_l is the cable loss, P_L is the path loss in dB.

The path loss P_L is calculated using the airport propagation model as follows:

$$P_L(d) = 99.8 + 10n \lg\left(\frac{d}{d_0}\right) \quad (8)$$

Where: the value of n is 2.3, d_0 is 462 m, and d is the distance from the phase center of the MLS antenna in km.

The radius of the MLS azimuth guidance coverage sector is about 41.7 km, and the DPSK data word signal and the scanning signal (3° beam width) transmitted by the azimuth station within this coverage, the transmitting antenna takes different gains. Since the MLS transmitting antenna uses line polarization and the satellite navigation signal uses circular polarization, polarization loss must be considered. Table 1 below gives the relevant parameters and their values for MLS signal power estimation, where “other loss” is a possible loss term.

In this paper, the interference situation between two services is considered, and the receiver is treated as unob-

structed from the interference source. In engineering applications, the satellite navigation receiver is generally installed on top of the aircraft, and we need to consider the influence factors such as airframe diffraction when evaluating the power of the MLS signal reaching the receiver.

3. Compatibility Methodology

3.1 Interference to MLS

In general, the MLS coverage area is near airports and some air routes. The satellite navigation signal is very weak by the time it reaches the MLS receiver after a long-distance spatial attenuation. However, approach landing is life safety-related, the interference of Cn-band navigation signals to MLS must be within acceptable limits.

ICAO gives the protection threshold for the MLS, it can be described as the aggregate PFD of satellite navigation signals falling on 5,030 MHz~5,150 MHz shall not exceed -124.5 dBW/m²/150 kHz, the PFD is defined as:

$$\text{PFD} = \frac{10^{0.1(EIRP_s - L_{atm})}}{4\pi d^2} \int_f^{f+150\text{kHz}} G(f)df \quad (9)$$

Where: d is the distance between the Earth receiver and the visible satellite in km, L_{atm} is the atmospheric loss, generally taken as 0.5 dB. $G(f)$ is the normalized power spectral density of the satellite navigation signal in the Cn-band. $EIRP_s$ is the effective isotropic radiated power, calculated by the equation as:

$$EIRP_s = (C_s/N_0)_{eff} + L_{rl} + N_0 + L_{fr} - A_r + L_{tro} \quad (10)$$

Where: L_{rl} is the receiver processing loss, taking the value of 6 dB, N_0 is the thermal noise power density, generally take the value of -174 dBm/Hz, L_{fr} is the Cn-band signal space transmission loss in dB, A_r is the receiver antenna gain in dBi, L_{tro} is the tropospheric attenuation, C-band tropospheric attenuation generally take the value of 5.9 dB, $(C_s/N_0)_{eff}$ is the Cn-band satellite navigation signal in 0.1 m code tracking accuracy.

3.2 Interference to Cn-Band Satellite Navigation Signal

The satellite downlink reception system mainly consists of antennas, feed sources, HF heads, transmission cables, power dividers, and satellite receivers. The receiver RF front-end processing module receives mixed signals, including all visible satellite signals and various electromagnetic field signals, and other interferences [24]–[26].

It is known that the interference signal will have an impact on the receiver expectation signal capture and other performance. This impact is related to the immediate branch, the branch correlator output a signal to interference plus noise ratio(SNIR) to evaluate it [27]–[30].

Skip the SNIR derivation process of the coherent and incoherent output of the immediate correlator, and treat the

interference signal as Gaussian white noise, the output carrier to interference plus noise ratio ρ of the immediate branch can be obtained as:

$$\begin{aligned} \rho &= \frac{C_s}{C_I + N} \\ &= \frac{P_0 \int_{-B/2}^{B/2} |H_B(f)|^2 G_0(f) G_C(f) df}{P_I \int_{-B/2}^{B/2} |H_B(f)|^2 G_I(f + \Delta f) G_C(f) df + I} \quad (11) \\ I &= N_0 \int_{-B/2}^{B/2} |H_B(f)|^2 G_C(f) df \end{aligned}$$

Where: P_0 is the navigation signal power, P_I is the interference signal power, and N_0 is the white noise power, all in dBW or dBm. $H_B(f)$ is the baseband frequency characteristic of the bandpass filter, which is set to the ideal case for calculation; $G_0(f)$ is the power spectrum of the navigation signal in the pre-integration time, $G_C(f)$ is the normalized power spectral density of the local reference signal, and $G_I(f)$ is the power spectrum of the interference signal in the pre-integration time.

When the interference signal is not considered, the carrier-to-noise ratio ρ_{SNR} is expressed as:

$$\begin{aligned} \rho_{SNR} &= \frac{C_s}{N} \\ &= \frac{P_0 \int_{-B/2}^{B/2} |H_B(f)|^2 G_0(f) G_C(f) df}{N_0 \int_{-B/2}^{B/2} |H_B(f)|^2 G_C(f) df} \quad (12) \end{aligned}$$

Then

$$\frac{P_0}{N_0} = \frac{\rho_{SNR} \int_{-B/2}^{B/2} |H_B(f)|^2 G_C(f) df}{\int_{-B/2}^{B/2} |H_B(f)|^2 G_0(f) G_C(f) df} \quad (13)$$

When considering both noise and interference:

$$\begin{aligned} \left(\frac{P_0}{N_0}\right)_{eq} &= \frac{\rho \int_{-B/2}^{B/2} |H_B(f)|^2 G_C(f) df}{\int_{-B/2}^{B/2} |H_B(f)|^2 G_0(f) G_C(f) df} \\ &= \frac{P_0 \int_{-B/2}^{B/2} |H_B(f)|^2 G_C(f) df}{P_I \int_{-B/2}^{B/2} |H_B(f)|^2 G_I(f + \Delta f) G_C(f) df + E I} \\ &= \frac{P_0}{P_I \frac{E I}{\int_{-B/2}^{B/2} |H_B(f)|^2 G_C(f) df} + N_0} \quad (14) \end{aligned}$$

$$E1 = N_0 \int_{-B/2}^{B/2} |H_B(f)|^2 G_C(f) df$$

$$E2 = \int_{-B/2}^{B/2} |H_B(f)|^2 G_I(f + \Delta f) G_C(f) df$$

Thus, the SSC can then be given by the expression of

$$SSC(\Delta f) = \frac{\int_{-B/2}^{B/2} |H_B(f)|^2 G_I(f + \Delta f) G_C(f) df}{\int_{-B/2}^{B/2} |H_B(f)|^2 G_C(f) df} \quad (15)$$

In Eq. (15): Δf is the frequency difference between the desired signal and the interfering signal in MHz.

From Eq. (14) and Eq. (15), the equivalent carrier-to-noise ratio based on the SSC is

$$\left(\frac{P_0}{N_0}\right)_{eq} = \frac{P_0}{P_I k(\Delta f) + N_0} \quad (16)$$

The SSC characterizes the degree of spectral overlap between the desired signal and the interfering signal and is one of the important parameters for evaluating radio frequency compatibility. In this paper, the value is calculated to evaluate the interference of MLS signals to satellite navigation signals from a spectral perspective. The equivalent carrier-to-noise ratio based on the SSC is proportional to the output carrier-to-noise ratio of the immediate correlator for both coherent and incoherent processing and can be used to evaluate the satellite navigation signal capture performance. Based on the empirical threshold of the carrier-to-noise ratio, the required separation distance value to avoid harmful interference will be calculated.

4. Ground Test and Analysis

4.1 Compatibility Test

The equipment used in the testing process includes RF unit, signal acquisition equipment, omnidirectional receiving antenna, mobile power supply, data processing equipment, and some auxiliary materials, some of them shown in Fig. 5.

The RF unit model is HN-SFSB-RF, which is used to convert the RF signal to an IF signal. The signal acquisition equipment model EXMC2102 consists of the acquisition, storage and control, clock, and other modules. To receive RF signals, an omnidirectional receiving antenna model R200500234 is equipped. A mobile power supply is used to power the device during signal acquisition. Auxiliary materials include materials such as laser range finders, cables, and adapters.

Limited by test conditions and test site, the navigation signal acquisition work and the MLS signal acquisition work were implemented independently of each other. The Cn-band satellite navigation downlink signal operates at 5022.93 MHz, its time-domain curves and power spectral



(a) RF unit.



(b) Signal acquisition equipment.



(c) Omnidirectional receiving antenna.



(d) mobile power supply.

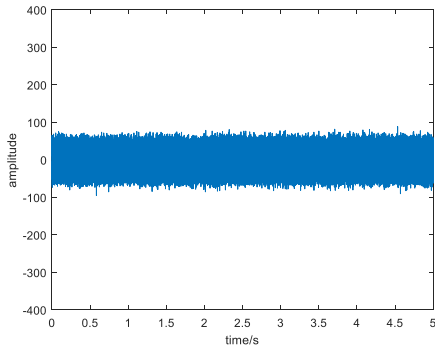
Fig. 5 Equipment used in the testing process.

density curves are shown in Fig. 6, with a sampling rate of 100 MHz, an acquisition bandwidth of 80 MHz, and an IIR filter at the receiver end (after down-conversion).

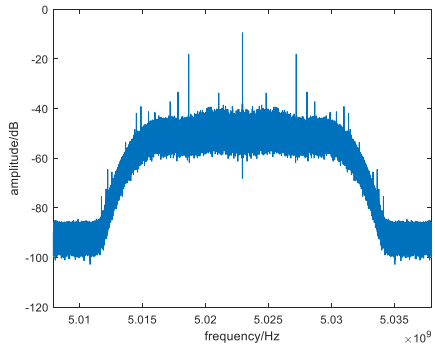
The MLS test was conducted at a military airfield where a runway configured with typical MLS equipment, at least an azimuth station, a precision DME, and an elevation station. The MLS signal acquisition points are set up as shown in Fig. 7.

During the test, the vehicle and testers should be kept from being between the azimuth station, elevation station, or back-azimuth station and the test equipment, thus affecting the test results. Care should be taken that the angle between the centerline of the runway and the red line in the figure ω meets the requirements, so as not to exceed the scanning signal coverage horizontal sector. The height of the azimuth equipment erected off the ground shall be taken into account.

Turn on the MLS device, an MLS signal at a distance of 2.7 km from the azimuth station of about 1 second in duration is acquired, and its time domain and power spectrum curve are shown in Fig. 8.

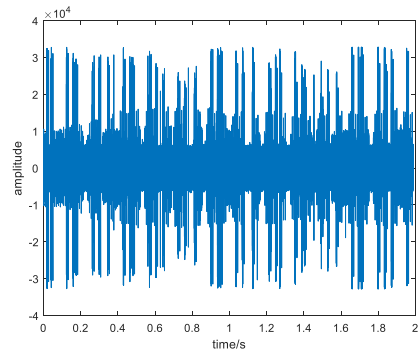


(a) Time-domain curves of Cn-band satellite navigation signal.

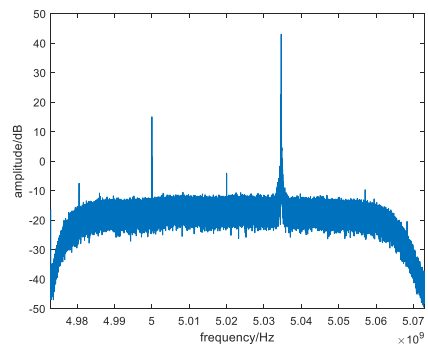


(b) PSD of Cn-band satellite navigation signal.

Fig. 6 Cn-band satellite navigation downlink signal.



(a) Time-domain curves of MLS signal.



(b) PSD of MLS signal.

Fig. 8 MLS signal at 2.7 km.

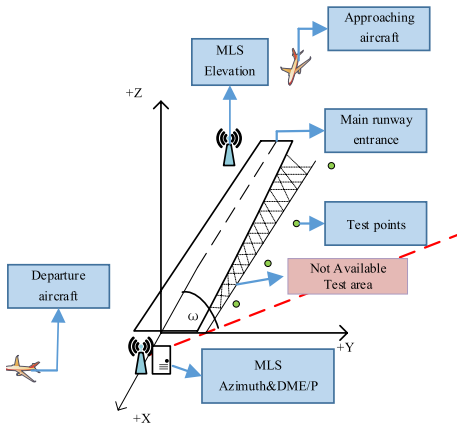


Fig. 7 Signal acquisition point setting.

4.2 Compatibility Test Results

PFD Values. During the test, there are 6 visible satellites in the MLS signal’s beam range. The satellite signal is operating at 5022.93 MHz with BPSK(10) modulation, with a receiving power of about -127.2 dBm, the distance between the satellite and the ground receiver is taken as 20,200 km. According to the compatibility analysis method described in Sect. 3.1, the total PFD ($\text{dBW}/\text{m}^2/150$ kHz) values, theoretical and numerical, of the Cn-band satellite navigation signal falling within the MLS band are recorded in Table 2.

From the calculation results in the table, it can be seen

Table 2 PFD values and interference results.

Parameters	BPSK(10)
Theoretical	-148.1036 dBW/m ² /150kHz
Measured	-149.5108 dBW/m ² /150kHz
PFD threshold	-124.5 dBW/m ² /150kHz
result	No harmful interference

that MLS signals do not cause harmful interference to Cn-band satellite navigation signals, and the theoretical results are consistent with the test results. There is an error between the theoretical and actual values, which is due to the low receiving power of the navigation signal. The captured signals are mixed with noise in the calculation, causing the actual value to be different from the theoretical value, which is an expected result.

Receiving power. When calculating the SSC as well as the equivalent carrier-to-noise ratio, MLS signals as interference signals should be classified into two categories, namely, DPSK data word signals and scanning signals. The former has a maximum duration of 9.3~15 ms, while the latter can be classified as high-gain narrowband continuous wave interference according to its generation principle. Figure 9 and Fig. 10 show the time-domain plots of the MLS DPSK data word signal and the scan signal collected at 1.7 km from the azimuth station.

Table 3 below gives the power of MLS DPSK data word signal and scanning signal for two sets of measured data at

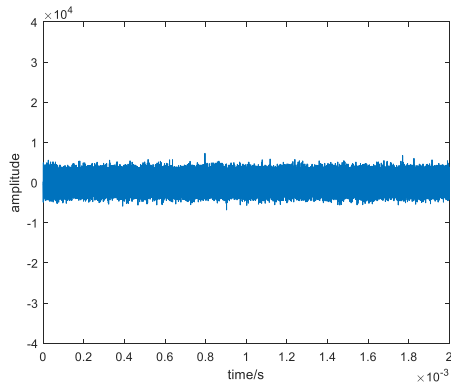


Fig. 9 MLS DPSK data word signal.

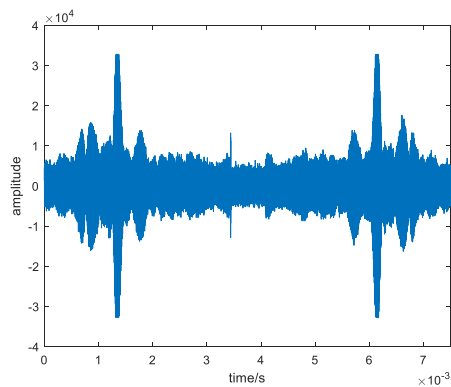


Fig. 10 MLS scanning signal.

Table 3 Receiving powers of MLS signal (dBm).

Parameters	DPSK signal		Scanning signal	
	1.7 km	2.7 km	1.7 km	2.7 km
Theoretical	-56.8	-60.4	-41.8	-46.4
Measured	-53.0	-57.4	-44.8	-46.0

1.7 km and 2.7 km from the azimuth station. The gain of the MLS azimuth antenna to the DPSK data word signal is taken as 8 dBi. The scanning signal beam width is 3°, and the gain to scanning signal is taken as 23 dBi.

SSC values. The bandwidth of the bandpass filter used at the transmitting end of the MLS signal is large (the pass-band is generally 60 MHz or more), which is to say the filter out-of-band rejection can be ignored when evaluating radio frequency compatibility with the Cn-band.

During the test, the MLS was operating at 5,031 MHz, and the carrier frequency of the Cn-band satellite navigation signal is 5022.93 MHz. Then the spectral separation coefficient values of the navigation signal with BPSK(10) modulation, and the MLS signal are recorded in Table 4, where the front-end filter bandwidth of the receiver is taken as the main flap bandwidth (20.46 MHz).

From the results in Table 3 and Table 4, it can be seen that the measured MLS signal power, as well as the SSC values, are relatively close to the theoretical values. The error

Table 4 SSC values.

	With DPSK signal		With scanning signal	
	1.7 km	2.7 km	1.7 km	2.7 km
Theoretical	-61.7		-62.1	
Measured	-56.9	-59.4	-61.6	-58.4

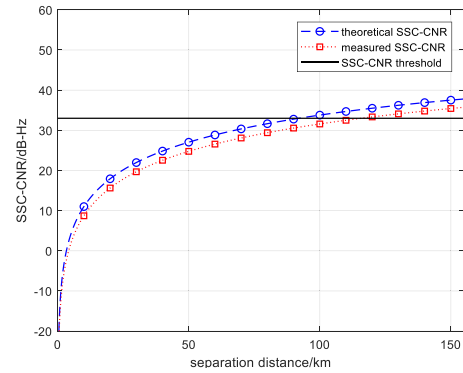


Fig. 11 SSC-CNR results with the separation distance changing (DPSK signal).

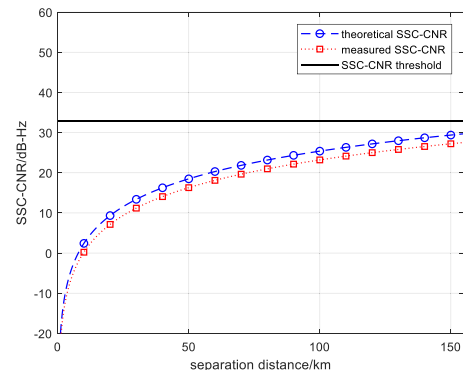


Fig. 12 SSC-CNR results with the separation distance changing (scanning signal).

sources are mainly some hardware losses and unexcepted signal transmissions of other communication systems in the environment.

To represent the interference between the two signals intuitively, the equivalent SSC-based carrier-to-noise ratio (SSC-CNR) is calculated below. In Fig. 11 and Fig. 12, the minimum carrier-to-noise ratio that allows the receiver to capture the navigation signal properly is taken as 33 dB-Hz [31], to give the required separation distance to avoid harmful interference.

The SSC-CNR values show an overall decreasing trend as the interfering signal (MLS) power increases, and the theoretical value is close to the calculated value of the test. With the receiver meeting the minimum carrier-to-noise ratio threshold of 33 dB-Hz, taking MLS DPSK data word signal as an example, the measured required separation between the navigation receiver and the MLS antenna phase center is 110.2 km, which means that the satellite navigation receiver

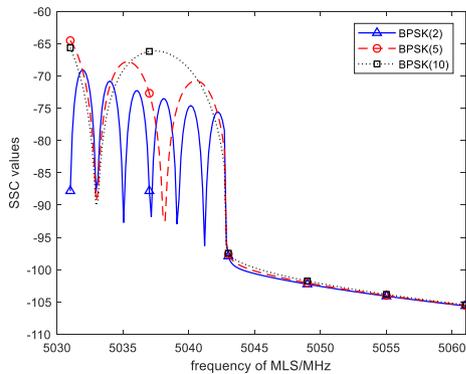


Fig. 13 SSC results with the center frequency of MLS DPSK signal changing.

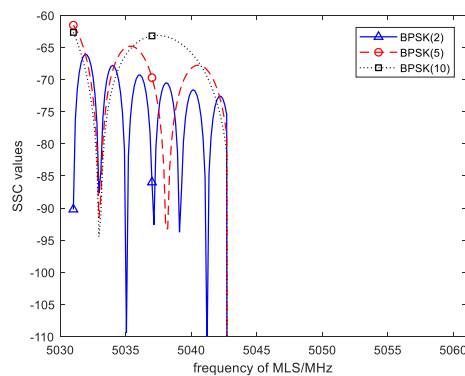


Fig. 14 SSC results with the center frequency of MLS scanning signal changing.

in this range will not be able to serve properly.

The operating bandwidth of MLS is wide and can reach 5,030 MHz~5,150 MHz in extended mode, which can be applied to numerous frequency points. To confirm the effect of changing the MLS operating frequency on the spectral compatibility, Fig. 13 and Fig. 14 plot the change of the spectral separation coefficient when the MLS DPSK signal and the scanning signal traverse the operating frequency from 5,030 MHz to 5,061 MHz, respectively, and the receiver front-end filter bandwidth is taken as 40 MHz.

From Fig. 13 and Fig. 14, it can be seen that with the right shift of the MLS operating frequency, the SSC values of the Cn-band navigation signal using the BPSK modulation method and the MLS signal show an overall decreasing trend. When the navigation signal is BPSK(2) modulated, the spectral separation curve has multi-valley characteristics and overall low spectral separation values, which means there are more frequency points MLS can be applied.

5. Conclusions

In this paper, preliminary tests and analysis for the radio frequency compatibility of Cn-band satellite navigation downlink signals and MLS signals are conducted, and the following conclusions are drawn. First, the downlink signal of the Cn-band satellite navigation system using BPSK(10)

modulation does not cause harmful interference to the international standard MLS. Navigation signals using other modulation methods require further analysis, which can be performed in the same way as in this paper. Second, the two kinds of guidance signals broadcast by the MLS have different degrees of influence on the navigation downlink signal reception. Due to the high gain characteristics of the scanning signal in the coverage sector, it brings stronger interference, in comparison, the DPSK signal brings weaker interference. The above interference can be avoided by a certain geographical interval. Finally, the radio frequency compatibility of the signals of the two systems can be greatly improved by adjusting the MLS operating frequency. The MLS operating frequency is very flexible with more than 200 operating channels and can take different operating frequencies for different runways. The above findings are an important part of the assessment of compatibility and interoperability between Cn-band satellite navigation systems and other primary systems in adjacent frequencies.

Acknowledgments

This work has been sponsored by the National Key R&D Program (2016YFB0502402) and the transversal projects of CAS (H04420210037).

References

- [1] R. Schweikert, T. Wörz, R. De Gaudenzi, A. Steingass, and A. Dammann, "On signal structures for GNSS-2," *International Conference on Human-computer Interaction with Mobile Devices & Services ACM*, vol.18, no.2, pp.271–291, 2014. DOI: 10.1002/1099-1247(200007/10)18:4/5<271::AID-SAT658>3.3.CO;2-P.
- [2] H.L. Trautenberg, T. Weber, and C. Schäfer, "GALILEO system overview," *Acta Astronautica*, vol.55, no.3–9, pp.643–647, 2004. DOI: 10.1016/j.actaastro.2004.05.046.
- [3] M. Irsigler, G.W. Hein, and A. Schmitz-Peiffer, "Use of C-band frequencies for satellite navigation: Benefits and drawbacks," *GPS Solutions*, vol.8, no.1, pp.119–139, 2004. DOI: 10.1007/s10291-004-0098-2.
- [4] G. Hein, M. Irsigler, J.A. Avilarrodriguez, et al., "Envisioning a Future GNSS System of Systems Part 3 A Role for C-Band?," *Inside GNSS*, pp.64–73, 2007.
- [5] A. Schmitz-Peiffer, L. Stopfkuchen, F. Soualle, et al., "Assessment on the use of C-band for GNSS within the European GNSS evolution programme," *21st International Technical Meeting of the Satellite Division of the Institute of Navigation*, vol.2, no.6, pp.637–646, 2008.
- [6] A. Schmitz-Peiffer, L. Stopfkuchen, F. Soualle, et al., "Architecture for a future C-band/L-band GNSS mission, Part 1: C-band services, space- and ground segment, overall performance," *Inside GNSS magazine*, pp.47–57, 2009.
- [7] J.H. Won, B. Eissfeller, B. Lankl, et al., "C-band user terminal concepts and acquisition performance analysis for european GNSS evolution programme," *Proc. 21st International Technical Meeting of the Satellite Division of The Institute of Navigation*, pp.940–951, 2008.
- [8] R. Avila, S. Wallner, J.H. Won, et al., "Study on a Galileo signal and service plan for C-band," *ION GNSS*, vol.2, no.5, pp.515–529, 2008.
- [9] M. Irsigler, G.W. Hein, B. Eissfeller, et al., "Aspects of C-band satellite navigation: Signal propagation and satellite signal tracking."

- Proc. ENC GNSS Conference, pp.27–30, 2002.
- [10] C. Fen, Y. Xuhai, L. Zhigang, C. Liang, and F. Chugang, "Signal biases calibration for precise orbit determination of the chinese area positioning system using SLR and C-band transfer ranging observations," *J. Navigation*, vol.69, no.6, pp.1234–1246, 2016. DOI: 10.1017/S0373463316000205.
- [11] X. Lu, H. Wu, Y. Bian, and Y. Hua, "Signal structure of China area positioning system," *Science in China Series G: Physics, Mechanics and Astronomy*, vol.52, pp.412–422, 2009. DOI: 10.1007/s11433-009-0061-x.
- [12] Z.Y. Li, Y. Bai, and X.C. Lu, "Research on radio frequency compatibility evaluation method of C_N band navigation signal," *J. Time and Frequency*, vol.42, no.01, pp.87–95, 2019. DOI: 10.13875/j.issn.1674-0637.2019-01-0087-09.
- [13] M.C. Niu, "Research on GNSS multi-frequency signal compatibility," Ph.D. Dissertation, Shanghai Jiaotong University, Shanghai, 2016.
- [14] M.H. Liu, X. Zhan, L. Wei, and M. Chen, "A compatibility analysis between GNSS and radio astronomy/microwave landing system in C band," *J. Aeronautics, Astronautics and Aviation*, vol.46, no.2, pp.102–107, 2014. DOI: 10.6125/13-0624-749.
- [15] M.H. Liu, "Study on C band satellite navigation signal architecture," Ph.D. Dissertation, Shanghai Jiaotong University, Shanghai, 2016.
- [16] R. Xue and Y.B. Zhao, *Design Theory and Key Technology of Multi-band Satellite Navigation Signal*, pp.101–120, Publishing House of Electronics Industry, Beijing, 2020.
- [17] R. Jia, B. Jiao, L. Zhao, et al., "Susceptible characteristics of signal-carrier frequency on BPSK system," *J. Radio Engineering*, vol.48, no.1, pp.17–21, 2018. DOI: 10.3969/j.issn.1003-3106.2018.01.04.
- [18] K. Prabu, D.S. Kumar, and R. Malekian, "BER analysis of BPSK-SIM-based SISO and MIMO FSO systems in strong turbulence with pointing errors," *Optik*, vol.125, no.21, pp.6413–6417, 2014. DOI: 10.1016/j.ijleo.2014.08.006.
- [19] S. Ma, Y.T. Li, J.B. Wu, T.W. Geng, and Z. Wu, "Performance analyses of subcarrier BPSK modulation over M turbulence channels with pointing errors," *Optoelectron. Lett.*, vol.12, pp.221–225, 2016. DOI: 10.1007/s11801-016-6054-x.
- [20] Y.X. Zhou, S. Lou, Z. Tang, T. Zhao, W. Zhang, "Tunable and switchable C-band and L-band multi-wavelength erbium-doped fiber laser employing a large-core fiber filter," *Optics & Laser Technology*, vol.111, pp.262–270, 2019. DOI: 10.1016/j.optlastec.2018.09.042.
- [21] G. Xie, *Principles of GPS and Receiver Design*, pp.251–255, Publishing House of Electronics Industry, Beijing, 2009.
- [22] W.R. Henry and R.J. Kelly, "Microwave landing system: The new international standard," *Advances in Electronics and Electron Physics*, vol.57, pp.311–410, 1981. DOI: 10.1016/S0065-2539(88)60365-0.
- [23] C.J. Dai, D.W. Wu, X.B. Zhao, Y.Q. Wang, J. He, and X. Zhang, "The analysis method of error of MLS based on replacement technology of main-lobe beaming," *Beijing University of Posts and Telecommunications*, vol.35, no.63, pp.28–31, 2012. DOI: 10.3969/j.issn.1007-5321.2012.02.007.
- [24] A.K. Bhattacharyya, "EMC analysis methods and computational models," *IEEE Antennas Propag. Mag.*, vol.39, no.6, pp.668–670, Dec. 1997. DOI: 10.1109/MAP.1997.646805.
- [25] G. Michael, J. Kirchner, and M. Herzig, "Development of software structure for integrated navigation receivers in shipping," *IFAC Proceedings Volumes*, vol.33, no.9, pp.407–412, 2000. DOI: 10.1016/S1474-6670(17)38178-8.
- [26] X. Chen, Y. Qiu, J. Tian, J. Zuo, X. Lu, C. Yang, L. Xu, and R. Zhao, "Quantification characterization technology of electromagnetic compatibility based on test results," *High Power Laser and Particle Beams*, vol.33, no.12, pp.72–80, 2021. DOI: 10.11884/HPLPB202133.210138.
- [27] L. Zhao, S.H. Gao, and L.S. Guo, "Compatibility of multi-frequency signal sampling for GNSS RF front-end," *Chinese Inertial Technology*, vol.18, no.3, pp.316–320, 2010.
- [28] W. Liu, S. Li, L. Liu, M. Niu, and X. Zhan, "A comprehensive

methodology for assessing radio frequency compatibility for GPS, Galileo and compass," *Proc. International Technical Meeting of the Satellite Division of the Institute of Navigation*, vol.7672.6, no.9, pp.943–954, 2010.

- [29] L. Liu, X. Zhan, W. Liu, and M. Niu, "Improved model of GNSS radio frequency compatibility assessment," *IEICE Electron. Express*, vol.8, no.6, pp.636–643, 2011. DOI: 10.1587/eleex.8.636.
- [30] Q.B. Xu, L.X. Zhang, Y.S. Meng, et al., "Analysis of the compatibility of the GNSS signal system," *J. Space Electronic Technology*, vol.8, no.2, pp.21–24, 2011. DOI: 10.3969/j.issn.1007-5321.2012.02.007.
- [31] X.F. Chen, X. Lu, X. Wang, and J. Ke, "Navigation signal design and ranging performance analysis of C_n band based on satellite-to-ground link," *J. Time and Frequency*, vol.44, no.2, pp.2132–2142, 2021. DOI: 10.13875/j.issn.1674-0637.2021-02-132-10.



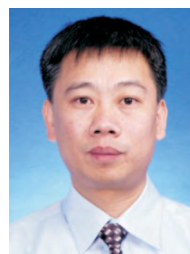
Ruihua Liu was born in 1965. He received his Ph.D. degree from Nanjing University of Aeronautics and Astronautics, China. He is currently a professor in the School of Electronic Information and Automation of Civil Aviation University of China. His main research interests are satellite navigation, integrated navigation and its application in civil aviation.



Yin Li was born in 1996. He received his B.S. degree from Northeastern University in 2018, and is now a graduate student in the School of Electronic Information and Automation, Civil Aviation University of China, with the main research interests in satellite navigation and microwave landing system.



Ling Zou was born in 1996. She received her B.S. degree from Civil Aviation University of China (CAUC) in 2019, and is now a graduate student in the School of Electronic Information and Automation of CAUC, where her main research interests are satellite navigation signal modulation methods.



Yude Ni was born in 1963. He received a double master's degree in Communication and Electronic Systems and CNS/ATM from Beijing University of Aeronautics and Astronautics in China in 1989 and from the National University of Civil Aviation in France in 2000. He is now a professor in the School of Electronic Information and Automation of Civil Aviation University of China. His main research interests are GNSS, CNS/ATM and PBN.